Research Article

Chemical Review and Letters
journal homepage: www.chemrevlett.com
ISSN (online): 2645-4947 (print) 2676-7279

Investigation of the antibacterial activity of phytosynthesized ZnO nanoparticles using *H. perforatum* extract

Roya Moeinzadeh[1], Malak Hekmati[1, *], Najmedin Azizi[2], Mahnaz Qomi[3,4], Davoud Esmaeili[5]

[1] *Department of Organic Chemistry, Faculty of Pharmaceutical Chemistry, Tehran Medical Sciences, Islamic Azad University, Tehran, Iran*

[2] *Department of Green Chemistry, Chemistry & Chemical Engineering Research Center of Iran, P.O. Box 14335-186, Tehran, Iran*

[3] *Active Pharmaceutical Ingeredients Research Center (APIRC), Tehran Medical Sciences, Islamic Azad University, Tehran, Iran*

[4]*Department of Medicinal Chemistry, Faculty of Pharmacy, Tehran Medical Sciences, Islamic Azad University, Tehran, Iran*

[5] *Department of Microbiology and Applied Virology Research Center, Baqiyatallah University of Medical Sciences, Tehran, Iran*

ARTICLE INFO

Article history:
Received 15 January 2024
Received in revised form 15 February 2024
Accepted 16 February 2024
Available online 16 February 2024

Keywords:
ZnO nanoparticles
Phytosynthesis
Hypericum perforatum
Antibacterial properties

ABSTRACT

In this work, a facile and fast phytosynthesis of zinc oxide nanoparticles (ZnO NPs) were reported employing an aqueous extracts of flowering shoot tips of *Hypericum perforatum* L. (*H. perforatum*) and zinc chloride as reactants. UV-Vis Diffuse reflectance spectroscopy (UV-Vis DRS), X-ray Diffraaction (XRD), Field emission scanning electron microscopy (FESEM), Transmission electron microscopy (TEM), Energy dispersive X-ray spectroscopy (EDS) and Fourier transform infrared spectroscopy (FT-IR) were applied to characterize the fabrication of ZnO NPs. TEM results show a semi-spherical shape and a size range of 14 nm for synthesized ZnO NPs and also represented UV-Vis absorption at 365 nm. The antibacterial property of phytosynthesized ZnO NPs and the aqueous extract of *H. perforatum* was also evaluated using the agar disc diffusion method (Kirby-Bauer test), minimum bactericidal concentration (MBC) and Broth micro-dilution method to determine the minimum inhibitory concentration (MIC). The bacteria examined in this study are *Methicillin-resistant Staphylococcus aureus* (*MRSA*), *Pseudomonas aeruginosa* (both common causes of nosocomial infections*)*, and *Bacillus subtilis*. Regarding the antibacterial properties of the synthetic samples, the best results were obtained with *H. perforatum*/ZnO NPs against *B. subtilis*. as follows: inhibition zone diameter at 1000 µg mL^{-1}, 18 mm, MIC and MBC values of 39.06 µg mL^{-1} and 78.12 µg mL^{-1}, respectively. Considering the favorable antibacterial activity of synthesized ZnO NPs using *H. perforatum* extract, they can be applied in bio-medicinal applications, particularly as nanobiotics.

1. Introduction

The nanotechnology field has progressively developed as scientists explore novel nanostructures. Among different nanostructures, nanoparticles possess exceptional physical and chemical characteristics, like a huge surface area, small particle size and also good reactivity [1]. Among metal oxides and metal nanoparticles, Ag NPs and ZnO nanoparticles have attracted researchers due to their excellent antibacterial properties as well as optical and catalytic properties [2]. Also, the use of natural polymers as polymer matrices to grow silver nanoparticles is even greater appealing due to they are biodegradable [3]. Zinc oxide NPs, as member of n-type semiconductor, have a high excitation energy (60 meV) and also a big band gap energy of approximately 3.3 eV [4-8]. The fabrication of ZnO nanostructures is dominated by various conventional physical and chemical methodologies [9-11]. However, such approaches need hazardous chemical reagents and stabilizers, conditions of temperature and high pressure,

∗ Corresponding author.; e-mail: mhekmatik@yahoo.com
https://doi.org/10.22034/crl.2024.435875.1281

expensive equipment, and are energy intensive, which do not in line with green chemistry guidelines. Thus to mitigate these challenges, biogenic routs are being developed and researched for the preparation of environmentally friendly and safe metal oxide NPs. The advantage of green synthetic processes is the utilize of eco-friendly reagents, cost- efficient and the production of less hazardous by-products [12-15]. In this method, different moieties like fungi, bacteria, plant and fruits extracts are implemented to fabricate ZnO NPs [16-20]. Among the various options, the green synthesis of ZnO NPs via plant extract have attracted considerable attention duo to its facile availability, eco-friendliness, simple set-up and cost-efficient approach, shorter duration and require less quantity of chemical solvents [1,21-22]. Nowadays, Numerous investigations have been conducted to prepare ZnO NPs via plant leaves/ or seed extract as capping/ reducing factors, owing to the disadvantages of chemically synthesized ZnO NPs. In recent researches, plant extracts of *Melia azedarach* [1], *Citrus jambhiri lushi leaves* [23], *Bergenia ciliata Rhizome* [24], *Punica Granatum* [25], *Echinochloa frumentacea* grains [26], *Ilex paraguariensis* [27], *Ficus benghalensis* [28], and *Syzgium cumini* leaves [29] have been applied for ZnO NPs fabrication. On account of these characteristics, ZnO NPs are extensively employed in numerous fields including novel gas sensors, biomedical equipment and optoelectronics [30-33], industry of cosmetic [34], anticancer [35], antimicrobial and fungicidal properties [36-37].

Today, nosocomial infections such as urinary tract infection, surgical site infection etc. are one of the main agents of death worldwide. They increase the length of hospitalization and also lead to higher costs and morbidity [38]. Multidrug-resistant strains are growing with overuse of antibiotics. Failure to treat diseases caused by bacteria is owing to their resistance to antimicrobial drugs. As a result, the discovery of new antibacterial agents seems imperative [39].In addition, studies show that almost two-thirds of deaths caused by antibiotic-resistant bacteria in Europe are caused by gram-negative infections [40]. Over the years, researchers have made great efforts to acquire antibacterial materials using various methods such as: addition of nitroalkane to chalcones using Michael addition reaction [41], synthesis of new antibiotic agent based on Mannich reaction [42], synthesis of novel amide derivatives [43]. Also Aldulaimi et al. [44] evaluated the antibacterial properties of fluorescent carbon nanoparticles (FC NPs) modified silicone denture soft liner. As mentioned, among different nanostructures, Ag NPs and ZnO NPs have attracted scholars due to their outstanding antibacterial. Several reports have shown that different types of silver nanoparticles have been used to inhibit fungi, bacteria, and viruses both in vitro and in vivo [45]. Also, biodegradable and antibacterial polymer films containing stable silver nanoparticles have been reported [46-48]. Several studies have also been conducted on the antibacterial properties of zinc oxide nanoparticles, especially against resistant bacterial strains [49]. Shokri et al. [25] used *P. granatum* fruit peel extract and zinc nitrate hexahydrate to synthesize ZnO NPs. The antibacterial activity of *P. granatum*/ZnO NPs was investigated using the broth microdilution method. The findings revealed that smaller size *P. granatum*/ZnO NPs exhibit better efficiency in inhibiting the growth of both Gram-negative and Gram-positive bacteria. Meanwhile, the cytotoxicity assay of *P. granatum*/ZnO NPs showed larger-sized particles have a slightly higher cytotoxicity against cancerous and normal cells.

In 2023, Dawar et al. used both microwave heating and conventional methods to prepare ZnO nanoparticles from the aerial roots of *Ficus benghalensis*. The antibacterial activities were studied by the agar well diffusion method against of Gram-positive and Gram-negative bacteria .The results demonstrated significant antibacterial activity of the synthesized ZnO NPs against the tested microorganisms [28]. Dhandapani et al. [1] prepared ZnO nanoparticles using leaf extract of *Melia azedarach* and zinc nitrate. Total antioxidant studies showed significant scavenger activity ranging from a minimum of 10.63% to a maximum of 54.97% . The antibacterial activities of green synthesized nanoparticles were tested against Gram-negative and Gram-positive bacteria using agar disc diffusion method and the broth micro-dilution method. The results indicated that phytosynthesized ZnO NPs have clear potential for nanomedicine formulation due to their promising antioxidant and antibacterial properties.

In another study, Pillai et al. [50] reported the synthesis of ZnO nanoparticles using the extracts of four different plants, including *Brassica oleracea var. Italica*., *Beta vulgaris*, *Cinnamomum tamala* and *Cinnamom verum*. The inhibition zone diameters of biosynthesized ZnO NPs against both Gram-negative and Gram-positive bacteria such as *Escherichia coli* and *Staphylococcus aureus*, respectively were evaluated. The antifungal properties of ZnO NPs were also shown against *Asper Gillus nigeri* and *Candida albicans* fungal stains. In general, the method was shown to be environmentally friendly, fast and cost-effective to synthesizing zinc oxide NPs as a potential antimicrobial agent against

multiple types of microbial species. In addition, there are many reports on the antibacterial properties of plants due to their non-toxicity, e.g *Matcha green* [51], *polyalthia lateriflora* [52], *Calopogonium mucunoides* [53], the essential oil of the fruits of *Phoenix dactylifera* [54]. Furthermore, *H. perforatum* is a flowering plant in the Hypericaceae family and is aboriginal to Europe, Australia, Maderia and west Asia. *H. perforatum* is considered as a principal medicinal plant around the world because it contains widespread types of secondary metabolites with significant medicinal activities [55]. This traditional plant is one of the most employed treatments for various disorders, like eczema, psychological disorders (specifically depression), inflammatory diseases, burn and skin wounds [56-57]. Furthermore, it has antioxidant, anti-diabetic, antitumor and antibacterial activities and is also used to hypotensive [57-58]. The significant components reported in aerial parts of *H. perforatum* include the following groups: prenylated phloroglucinols (hyperforin), flavonoids (hyperoside, quercetin, isoquercitrin, rutin), phenolic acids (neochlorogenic acid, chlorogenic acid), naphthodianthrones (hypericin, pseudohypericin) [56-57,59].

In this work, we describe a facile, rapid and cost-effective fabrication of ZnO NPs as a green synthesis method using aqueous extract of *H. perforatum* as stabilizing and capping factors. The physico-chemical characteristics of as-prepared nanoparticles were studied. The antibacterial activity of both the extract and the phytosynthesized ZnO NPs was also evaluated against *MRSA, P. aeruginosa* (both common causes of nosocomial infections) and *B. subtilis* using the agar disc diffusion method, MBC and Broth micro-dilution method to determine MIC.

2. Experimental

2.1. Materials and Methods

2.2. Chemicals

Zinc chloride ($ZnCl_2$. $2H_2O$), sodium hydroxide, were buyed from Merck (Germany) chemical company. Reagents applied in the present investigation were of pure and analytical grade. Deionized water was utilized in experiments.

2.3. Plant material collection

Flowering shoot tips of *H. perforatum* were collected from Bagh Firuze, village of Firuz Bahram (Tehran province, Iran) in June 2019. The voucher specimen was placed in the herbarium of the Faculty of Pharmaceutical Sciences, Tehran Medical Sciences, Islamic Azad University (Tehran, Iran) under code number of 273-PMP/A.

2.4. Preparation of aqueous extract of Hypericum perforatum

Flowering shoot tips of *H. perforatum* were first washed with water of tap and finally with Deionized Water (DI H_2O). The washed plants were dried in the shade and then ground. The obtained powder was soaked in DI water in a ratio of 1:10 at room tamperature. Then the mixture was heated and agitated during 1 hour and then shaken at room temperature. The resulting extract (a brown solution) was filtered and stored in a refrigerator at 4˚C. Additionally, part of the obtained aqueous extract was lyophilized (Christ Alpha 1-2, Germany) at -50 ˚C. The resulting brown powder was kept at room ambient for later use.

2.5. Biosynthesis of ZnO nanoparticles

100 mililiters of the aqueous extract of *H. perforatum* was combined with 50 ml of $ZnCl_2.2H_2O$ (0.1 M). The reaction mixture changed color (from brown to yellow-green) when the solution of 5 M NaOH was used to achieve a final pH of approximately 9.5. The mixture of reaction was heated and agitated at 80 ˚C for 1 hour. The resulting mixture was then cooled to ambient temperature and centrifuged (10 min, 10000 rpm). The precipitate was rinsed 3 times with DI H_2O in a centrifuge (10000 rpm, 10 min) and dried for 1 h in an oven. A dark brown precipitate was attained and after that this resulting precipitate was annealed at 500 ˚C for 3 hours. Pale white precipitate was obtained as the final product. *H. perforatum*/ZnO NPs were collected and stocked at ambient temperature for further experiments.

2.6. Characterization

The phytosynthesised ZnO NPs were confirmed through UV-Vis DRS in the range of 300-800 nm (Shimadzu-2550, Japan). FT-IR spectra were obtained for as-obtained samples in the range of 400-4000 cm^{-1} via an Avatar model FT-IR Spectrometer (Thermo, USA) to testify the functional groups. The structural and surface morphological features of the prepared nanoparticles were surveied using FESEM (Zeiss SigmaVP, Germany). Elemental analysis of the prepared samples was also performed by EDX. Biosynthesized ZnO NPs were subjected to X-ray diffraction analysis (XRD) with a Malvern, X'pert Pro diffractometer equipped with Cu Kα radiation (λ= 0.15406 nm) at 2θ range from 5◦ to 80◦. The shape and size of phytosynthesised ZnO NPs were also investigated by analyzing TEM images (Zeiss EM10C, Germany).

2.7. Antibacterial activity study

The bacterial strains applied in this study were collected from the Department of Microbiology and Applied Virology Research Center, Baqiyatallah University of Medical Sciences, Tehran, Iran. Among the microorganisms were two gram-positive bacteria; *Methicillin-resistant Staphylococcus aureus (MRSA), Bacillus subtilis (ATCC 6633)* and gram-negative bacteria; *Pseudomonas aeruginosa* (*PAO1*).

2.7.1. Agar disc diffusion method

The agar disc diffusion method has been used to define the susceptibility of microorganisms to as-obtained samples (Kirby-Bauer). First, bacterial suspensions for each tested bacterium were prepared with sterile saline (0.9% sodium chloride) and their cloudiness was adapted to standard solution of 0.5 McFarland's at a concentration of 1.5×10^8 CFU/ml. In petri dishes, the bacterial suspension was transferred to Mueller-Hinton Agar (MHA) medium and spread equally on the surface of the medium (grass culture) with a sterilized cotton swab. Then blank paper discs (diameters 6 mm) containing 25 µL of extracts and synthesized ZnO nanoparticles (at concentrations of 250, 500 and 1000 µg/mL) were placed on the inoculated medium. The plates were incubated for a duration of 20 hours at 37 ˚C, following which the diameter of the inhibition zone (mm) was investigated. Furthermore, Gentamycin standard discs (10 µg) were employed as control. Experiments were accomplished in triplicate.

2.7.2. MIC and MBC studies

Minimum inhibitory concentration (MIC) studies of extracts and fabricated ZnO NPs were achieved using a Clinical and Laboratory Standards Institute (CLSI) based Broth micro-dilution assay. This was performed using sterile 96-well microplates. All wells were filled with100 µL of Muller Hinton Broth (MHB). Then,100 microliters of the stock solutions from the synthesized samples were poured into the first well of each row in the microplate. Two-fold serial dilution of these stock solutions was done in 96-well microplates. The cloudiness of the bacterial suspensions was adapted standard solution of 0.5 McFarland's. Then 10 microliters of every diluted microbial suspension was transferred to all wells, so that after inoculation, every well included nealy 5×10^5 CFU /ml (CLSI 2015). Wells of control were filled with only MHB and solutions from synthesized samples (negative control) and also only with MHB and bacterial suspensions (positive control). After that, the microplates were located in an incobator for a duration of 20 hours at 37 ˚C. The MIC was then determined as the lowest concentration of extracts and synthesized zinc oxide nanoparticles that inhibited visible bacterial growth. On the other hand, the minimum bactericidal concentration (MBC) complements the MIC value. Each turbidity-free well corresponding to the MIC was cultured separately on Muller-Hinton agar medium. Then all the plates were incubated for a duration of 20 hours for MBC determination. MBC was then distinguished as the lowest concentration of the synthesized samples that prevented bacterial growth. Experiments were accomplished in triplicate. Additionally, Gentamycin was employed as a control.

3. Results and discussion

3.1. Phytosynthesis of ZnO nanoparticles using H. perforatum and possible mechanism

Phytosynthesized ZnO NPs are persistent and vary in shape and size. Some of the main factors affecting the different morphology and size of phytosynthesized ZnONPs may depend on the change in thermal treatment temperature, variations of pH, reaction time, zinc salt and extract concentration [60-61]. By increasing the extract concentration to a fixed amount of zinc precursor, the particle size decreases [62], particle size increases by increasing the concentration of Zn precursors without changing extract concentration [63], an increase in pH decreases particle size and agglomeration [20,64] as the calcination temperature increases, the crystallinity improves and the particle size increases [65-25]. Calcination temperature can also affect particle morphology. Sukri et al. [25] used *P. granatum* fruit peel extract for phytosynthesized ZnO NPs. They reported spherical structures in samples calcined at 500 °C, while hexagonal structures were also seen in samples calcined at 700 °C. The plant extracts contain different biomolecules, the compound and concentration of which can differ according to type of the plant. Considering the possible concurrent involvement of several bioactive molecules in the synthesis, the exact mechanism of the preparation of zinc oxide NPs using plant extracts is not known [61]. Many researchers believe that the possible mechanism is not related to the reduction of Zn^{2+} to zinc element and then oxidation in air at high temperature. Instead, Zn^{2+} forms a complex structure with bioactive molecules through polar functional groups. The complex is then thermally decomposed using calcination, releasing the ZnO nanoparticles, followed by particle growth, finally giving the observed capped and stabilized ZnO nanoparticles [27, 60-61, 66].

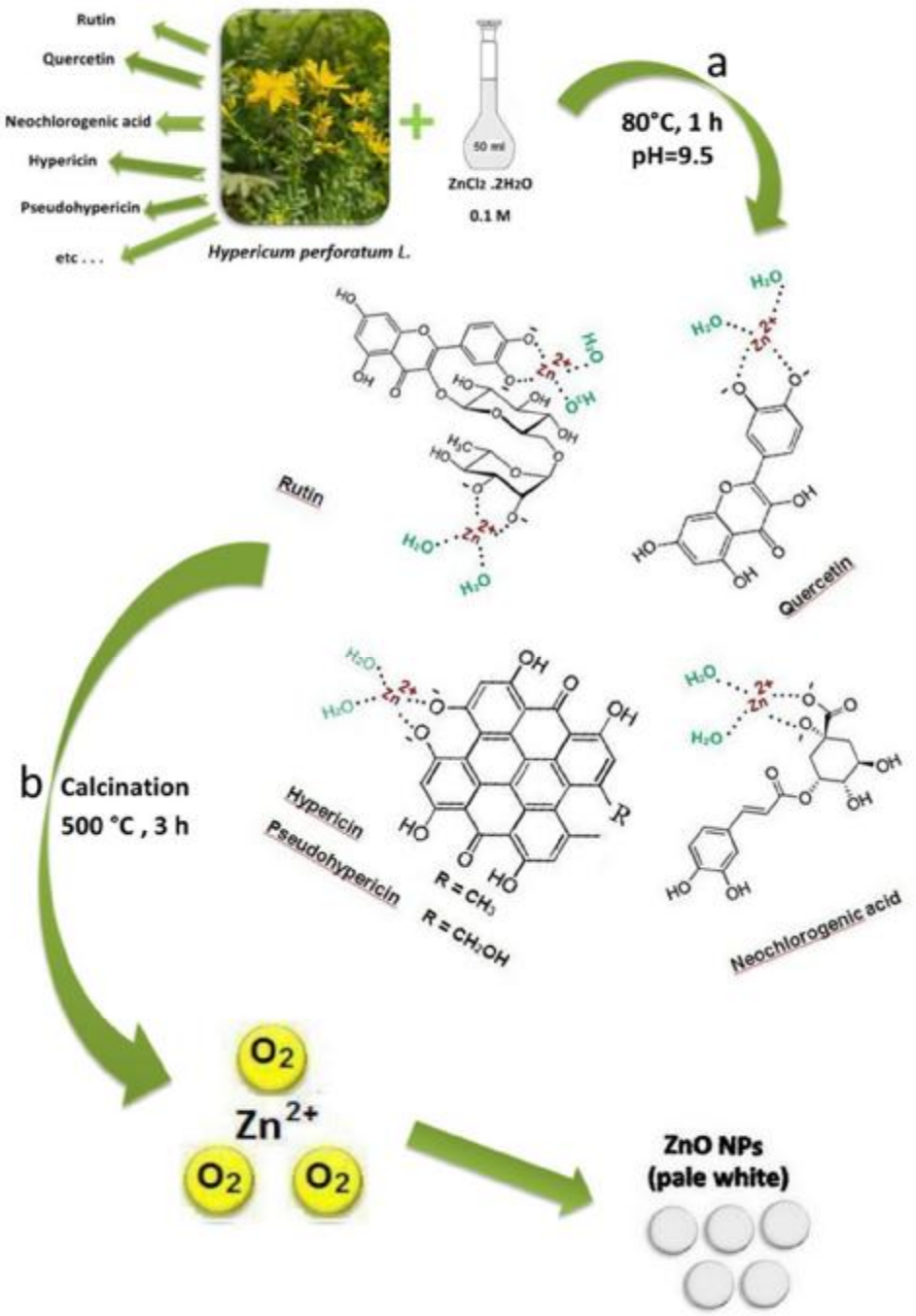

Fig. 1. Schematic diagram for synthesis of ZnO NPs using *H. perforatum* extract, a) interaction of Zn^{2+} ions with water and main compounds in *H. perforatum*, b) calcination of coordinated complexes and formation of *H. perforatum*/ZnO NPs.

In the current research, ZnO nanoparticles were obtained using an aqueous extract of flowering shoot tips of *H. perforatum*.

The most significant phytochemical components of *H. perforatum* have been isolated from the aerial parts of *H. perforatum*, including rutin, hyperforin, hyperoside, isoquercitrin, quercetin, neochlorogenic acid,

chlorogenic acid, hypericin and pseudohypericin [56,59]. These are compounds like flavonoids and polyphenols have hydroxyl groups or atoms with lone pair electrons like oxygen. They are better known as antioxidants and can neutralize free radicals and reactive oxygen species [67]. When aqueous extract of *H. perforatum* was heated with solution of $ZnCl_2.2H_2O$ (pH= 9.5) at 80 ˚C for 1 hour, the lone pair electrons of polar functional groups in aqueous extract like –OH, can occupy two orbitals of the Zn^{2+} ions and make coordinated complexes with positively charged zinc ions. Then resulting dark brown precipitate was annealed. Infact, when this precipitate is placed in muffle furnace at 500 ˚C for 3 hours, this action causes the release of carbon and its combustion, and most of the phytochemical components (Primary and secondary metabolites) of *H. perforatum* are removed. In addition, ZnO nanoparticles were formed via calcination of these complexes. FTIR analysis (Fig. 3c) revealed residues of phytochemical components of plant in *H. perforatum*/ZnO NPs. They played a fundamental role as capping and stabilizing factor in the phytosynthesis of ZnO NPs. Furthermore, these antioxidant components of *H. perforatum* also impeded the agglomeration of ZnO NPs via adhering to the surface of ZnO NPs and control the measure of nanoparticles. All these steps are shown schematically in Fig. 1.

3.2. UV-Vis DRS spectroscopy

Phytosynthesized ZnO NPs were evaluated using UV-Vis DRS in a range from 300-800 nm. The UV-Vis spectrum of ZnO NPs reveals an excited absorption peak at 365 nm (Fig.2). Similar UV-Vis results were also announced for other phytosynthesized zinc oxide NPs [27,68]. Due to the intrinsic band gap, when the excited electrons move from the valence bands to conduction bands, we can recognize the characteristic absorption peak of ZnO NPs [25]. The wavelength value reduces due to the decrease in the size of Zinc oxide NPs (blue shift) and the absorbance also decreases [25,27,69].

3.3. Fourier transform infrared (FTIR) spectroscopy

FTIR measurements were performed to distingush the potential biomolecules of the *H. perforatum* extract responsible (Fig. 3a). prenylated phloroglucinols (hyperforin), flavonoids (rutin, hyperoside, isoquercitrin), phenolic acids (neochlorogenic acid), naphthodianthrones (hypericin) are the most important constituents of *H. perforatum* [57,59]. In the FTIR spectrum of aqueous extract of *H. perforatum*, wide peaks between 3200-3600 cm^{-1} correspond to O–H stretching vibrations of phenols, alcohols and carboxylic acids.

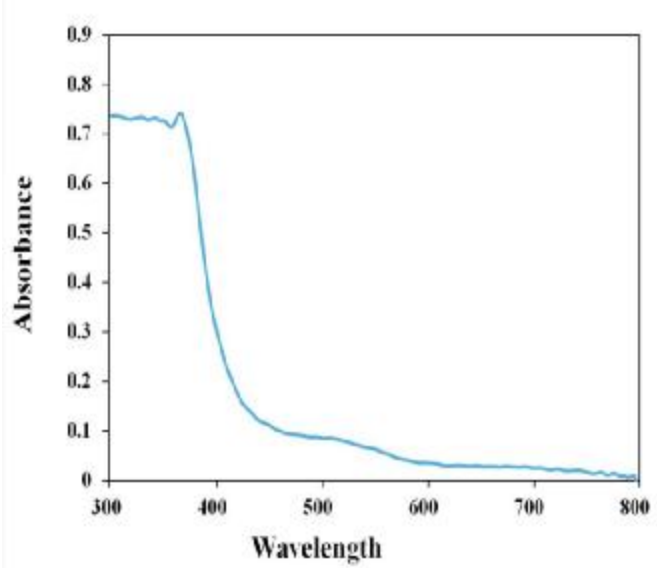

Fig. 2. UV-Vis DRS absorption spectra of phytosynthesized ZnONPs at 500 ˚C.

Bands at 3005 cm^{-1} and 2918 cm^{-1} show the C-H stretching of the alkene (both aromatic) and alkane respectively. Characteristic bands at 1624 -1732 cm^{-1} attributed to C=C aromatic stretching and vibration of –C=O groups of carboxylic acids, ketones and esters. The peak at 1456 referred to C=C aromatic stretching. The bands observed at 1076 cm^{-1} are due to C-O bond stretching of carboxylic acids, esters and alcohols. Figure 3c depicts the FT-IR analysis of *H. perforatum*/ZnO NPs. The peaks of the metal oxygen bond are between 400 and 600 cm^{-1} [70]. According to Figure 3c, the FT-IR spectrum manifest a characteristic peak at 451 cm^{-1} owing to the Zn-O vibrations [68]. Also the characteristic band at 3553 cm^{-1} represents the O-H functional group stretching vibrations of carboxylic acids, phenols and alcohols. The bands perceived at 1051 cm^{-1} attributed to C-O bond of esters, carboxylic acids, ethers and alcohols. The presented functional groups in FT-IR measurement (Fig. 3c) illustrated that these *H. perforatum* metabolites played a fundamental role as capping and stabilizing factor in the phytosynthesis of ZnO NPs. The residues of plant metabolites impeded the agglomeration of ZnO NPs via adhering to the surface of ZnO NPs. Also the FT-IR spectra of annealed ZnO NPs shows distinct characteristics at 451 cm^{-1} when compared with the FT-IR analysis of biosynthesized ZnO NPs before annealing process (Fig. 3b & 3c).

3.4. XRD analysis

According to Figure 4, the XRD pattern of annealed ZnO nanoparticles is depicted. The important diffraction peaks of ZnO nanoparticles at 2θ values of 31.84 ˚, 34.46 ˚, 36.27 ˚, 47.56 ˚, 56.69˚,62.97 66.50, ˚ 68.09˚ and 69.20 ˚ which can be attributed to the (100), (002), (101), (102), (110), (103), (200), (112) and (201) planes of the hexagonal form of ZnO, which proves the fabrication of Zinc oxide NPs [71-72]. The observed diffraction peaks correspond to the standard reference powder diffraction pattern accounted for hexagonal ZnO NPs (JCPDS no 36-1451) [27]. The existence of sharp and strong diffraction peaks represents that the annealed ZnO NPs posses excellent crystallinity. Furthermore, the crystallite size (D) of the annealed ZnONPs was computed via the Debye-Scherer equation: $D=K\lambda/\beta\cos\theta$ where, λ is the applied X-ray wavelength (0.15406 nm), D is the crystallite size of NPs (nm), K is the Scherer shape factor (0.9), β is the full width at half maximum (FWHM) in radians and θ is the angle of Bragg diffraction. According to this, the mediocre crystallite size of annealed ZnONPs was computed to be 11.76 nm, which is consistent with TEM observations.

3.5. FE-SEM/TEM and the EDS/Map studies of H. perforatum/ZnO NPs

FESEM is an principal tool for studying size distribution, surface morphology and fundamental structural characteristics. So far, various morphologies have been accounted in the production of ZnO NPs through the utilization of diverse plant extracts [27,60]. The shape and size of phytosynthesized ZnO NPs vary depending on the zinc salt and extract used [27]. The FESEM micrograph of biosynthesized ***H. perforatum/ZnO NPs*** revealed that the nanometer-scale sample was fabricated in a semi-spherical shape. Figure 5 and Figure 6 represent FESEM images of *H. perforatum*/ZnO NPs without calcinations and annealed *H. perforatum*/ZnO NPs at 500˚C, orderly. The EDS/Map technique was recorded and depicted for *H. perforatum*/ZnO NPs in Figure 7 (a & b) and affirms the presence of Zn, O and C elements in the physico-chemical composition of the biosynthesized ZnO NPs. The presence of carbon can be originated from a plant extract. Furthermore, the shape and morphological properties of the phytosynthesized ZnO NPs were assessed via transmission electron microscopy (TEM). A quasi-spherical particle morphology can be distinguished in the annealed ZnO NPs sample (Figure 8 a & b). Aditionally, the particle size distribution histogram defined from the TEM images showed a mean size of *H. perforatum*/ZnO NPs of 14 nm at 500˚C (Figure 8 c). Furthermore, TEM and FESEM micrographs showed that the obtained samples were surrounded and stabilized by a thin protective layer containing biomolecules of *H. perforatum* extract.

3.6. Antibacterial properties

P. aeruginosa is a rod-shaped gram-negative bacterium. S. aureus and B. subtilis are both Gram-positive bacteria, but one is round and the other rod-shaped. Among the strains of S.aureus, MRSA is genetically distinct from the others. MRSA and P. aeruginosa are among the main operative of nosocomial infections and also have high resistance to common antibiotics. These opportunistic pathogens contribute greatly to burn infections and are the most important reasons of death in patients, especially in the intensive care unit (ICU) [73]. A number of studies have shown that ZnONPs are not toxic in human cells [74]. However, ZnONPs can conveniently interact with biological molecules and can be used as an antibacterial agent. They have antibacterial properties and treat bacterial infections caused by various causes, such as high surface-to-volume ratio, reduced particle size, increase of particle surface reactivity, properties of physicochemical [75-76]. One of the most important factors influencing the susceptibility of bacteria to nanomaterials is the particle size [25]. ZnO NPs with an average size of 30 nm can eliminate the membrane integrity through direct contact with lipid bilayers [75].

3.6.1. Evaluation of the inhibition zone diameter of prepared samples

Here, the antibacterial properties of *H. perforatum* aqueous extract and *H.perforatum*/ZnO NPs at various concentrations (250,500,1000 μg/mL) were studied according to the inhibition zone diameter via agar disc diffusion approach against three different microorganisms like *MRSA*, *B. subtilis*, and *P. aeruginosa*. When the concentration of the drugs (plant extract and as-prepeard ZnO NPs) increases, the inhibition zone intensifies against all bacteria, and as a result, the effectiveness of drugs also increased. Also, examination of the inhibition zone of all drugs showed that the lowest amount was against *P. aeruginosa* and the largest against *B. subtilis*.

As shown in Table 1, the highest inhibition zone was achieved for *H. perforatum*/ZnO NPs against *B. subtilis* (18 mm), followed by *MRSA* (13 mm) and *P. auroginosa* (10 mm) at 1000 μg mL^{-1}. The findings also presented that *MRSA* and *B. subtilis* are more susceptible to phytosynthesized ZnO NPs than *P. aeruginosa*. The resistantness of Gram-negative bacteria

to antibiotics owing to their impenetrable cell walls is higher than that of Gram-positive bacteria. Additionally, according to the results obtained, the zone of inhibition of *H. perforatum* aqueous extract against *B. subtilis* at 1000 µg mL^{-1} was 10 mm, but no results

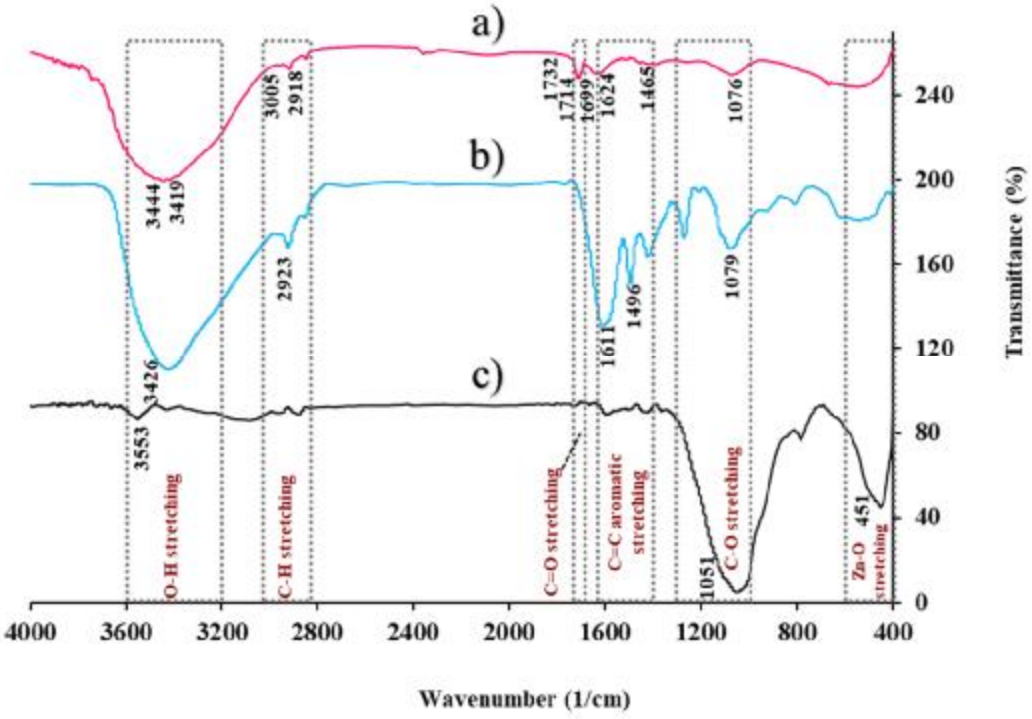

Fig. 3. FT-IR spectra of a) *H. perforatum* aqueous extract, b) *H. perforatum*/ZnO NPs without calcination and c) annealed *H. perforatum*/ZnO NPs at 500˚C.

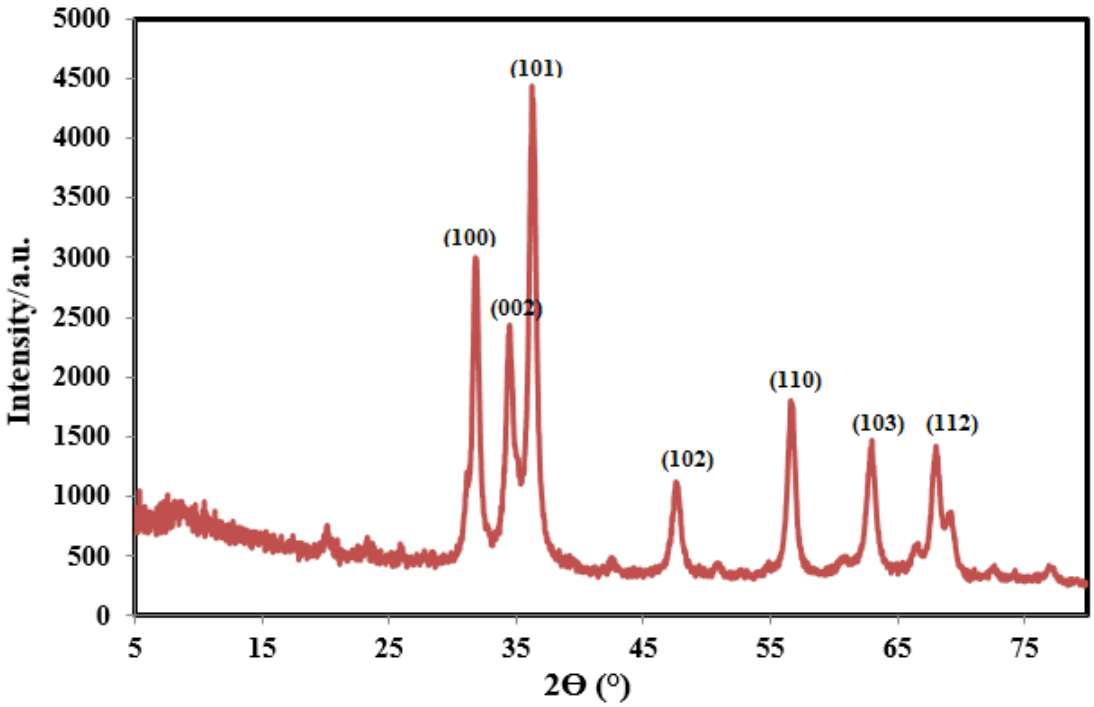

Fig. 4. XRD pattern of *H. perforatum*/ZnO NPs (annealed at 500˚C)

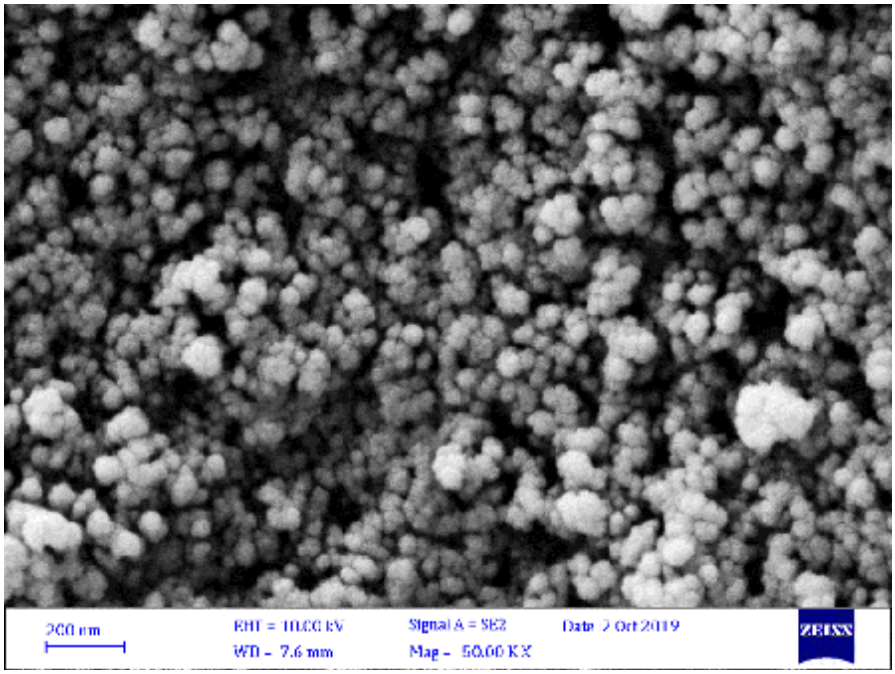

Fig. 5. Fesem images of *H. perforatum*/ZnO NPs befoe calcination.

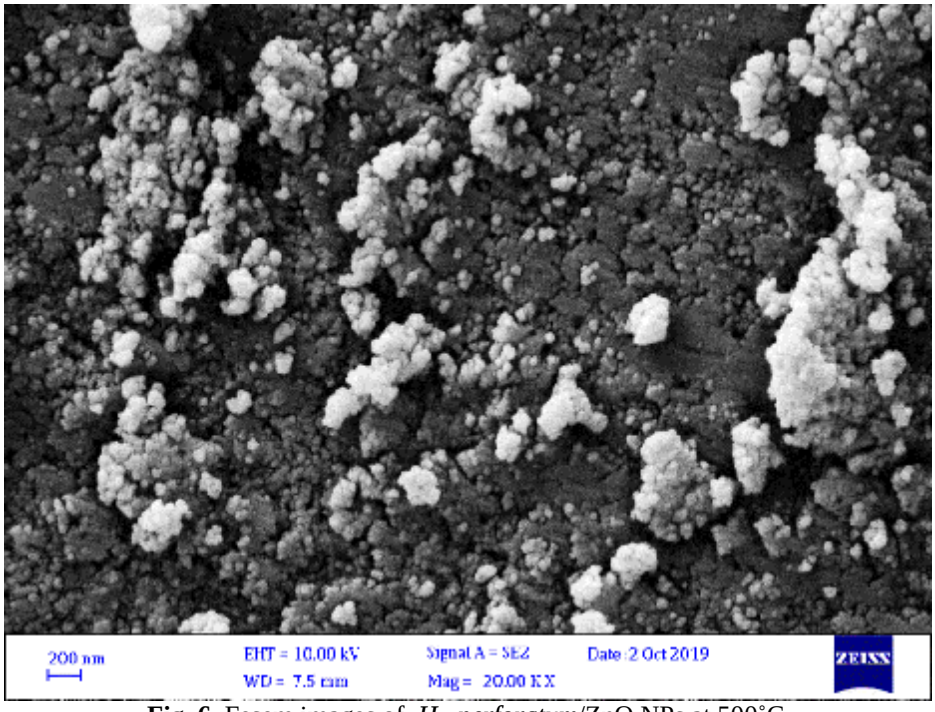

Fig. 6. Fesem images of *H. perforatum*/ZnO NPs at 500˚C

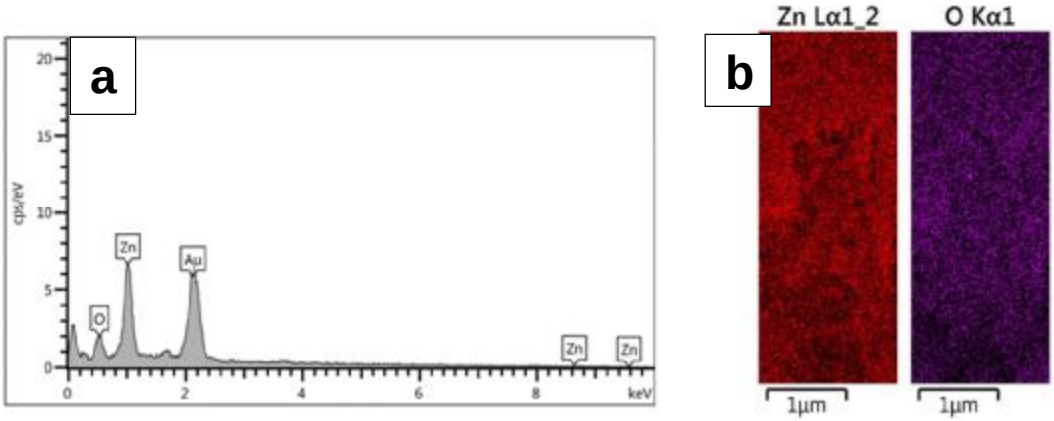

Fig. 7. a) EDX patterns and b) Mapping of *H. perforatum*/ZnO NPs at 500˚C

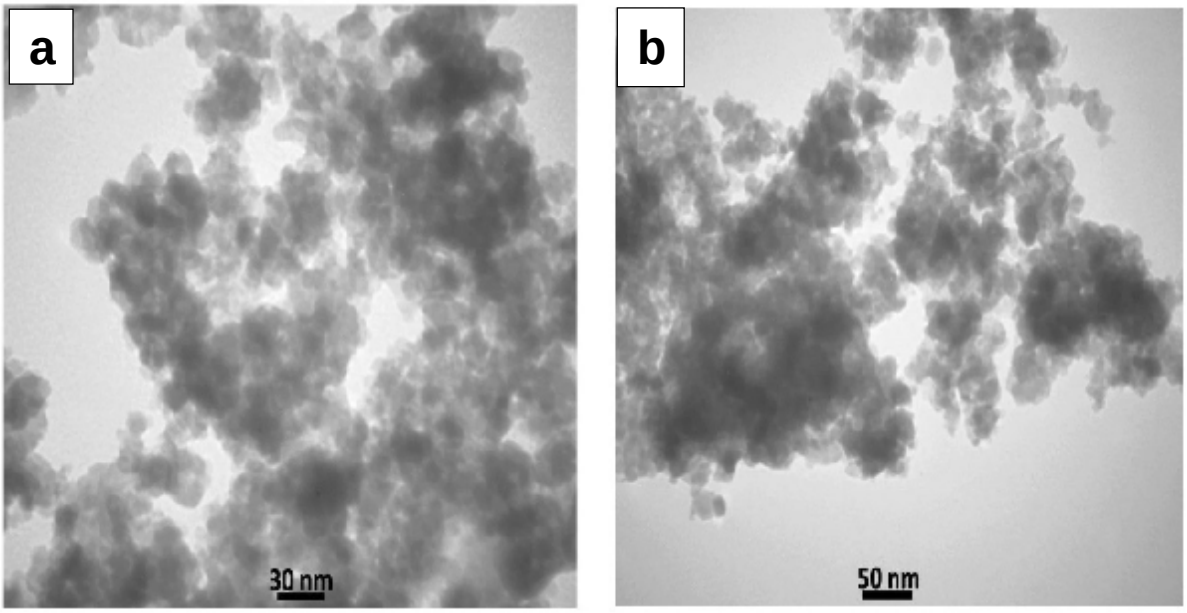

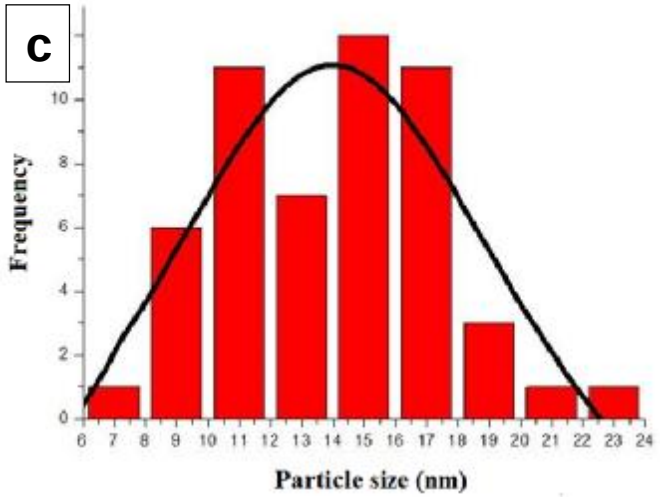

Fig. 8. TEM micrographs of *H. perforatum*/ZnO NPs at 500˚C (a & b), the particle size distribution histogram defined from the TEM images (c).

Table 1 Inhibition zone of *H. perforatum* extract and *H. perforatum*/ZnO NPs against *MRSA*, *P. aeruginosa* and *B. subtilis* using disc diffusion method

Samples	Concentration (μg mL^{-1})	Inhibition zone (mm)		
		Microorganisms		
		MRSA	*B. subtilis*	*P. aeruginosa*
H. perforatum aqueous extract	250	no Zone	8	no Zone
	500	no Zone	9	no Zone
	1000	no Zone	10	no Zone
H. perforatum/ZnO NPs	250	11	12	7
	500	12	16	8
	1000	13	18	10
Gentamycin	10 μg/disc	20	26	17

Table 2 Minimum inhibitory and minimum bactericidal concentrations of *H. perforatum*/ZnO NPs and *H. perforatum* extract against *MRSA*, *P. aeruginosa* and *B. subtilis*

Studied Microorganisms	*H. perforatum*		*H. perforatum*/ZnO NPs		Gentamycin	
	MIC*	MBC*	MIC	MBC	MIC	MBC
MRSA	2500	2500	156.2	312.5	0.292	0.585
B. subtilis	2500	2500	39.06	78.12	0.146	0.292
P. aeruginosa	-	-	625	625	18.78	37.5

MIC and MBC values are described in terms of μg/mL

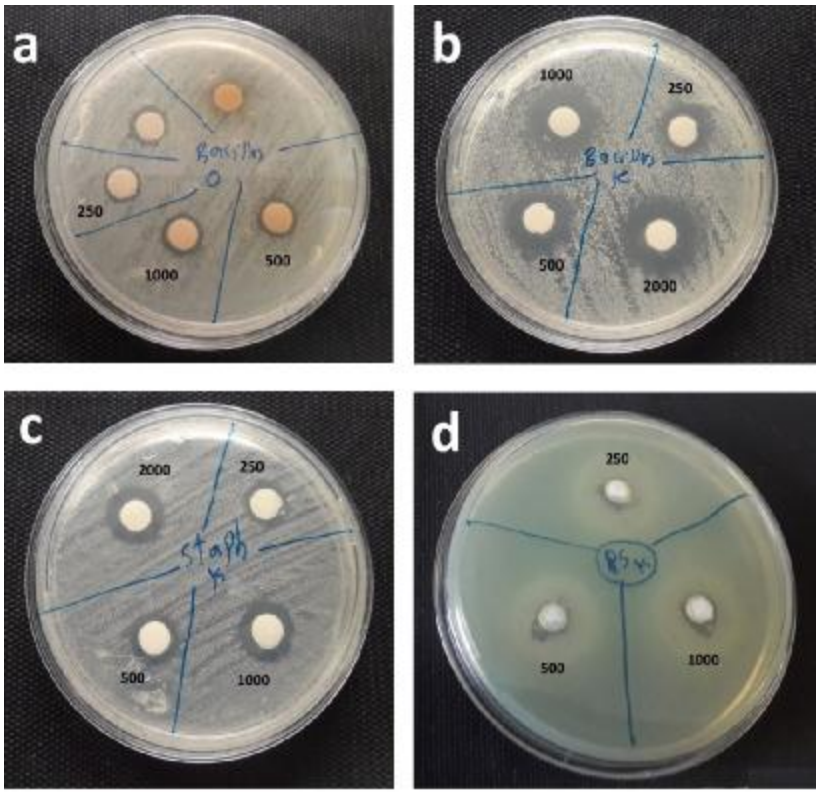

Fig. 9. Inhibition zone of a) *H. perforatum* extract against *B. subtilis* and Inhibition zone of photosynthesized ZnO NPs against b) *B. subtilis*, c) *MRSA*, d) *P. aeruginosa.*

were obtained for other bacteria. In other words, *P. aeruginosa* and *MRSA* are resistant to the extract, while *B. subtilis* is a semi-susceptible bacterium. The inhibition zone of samples against the selected microorganisms were presented in Fig.9. The outcomes are like to those reported of Mahendra et al. [77], which showed that biosynthesized ZnO NPs were more intense antibacterial properties than plant extract. In another report [66], the antibacterial property of biosynthesized ZnO NPs was investigated via *Rosa canina*. The zones of inhibition of ZnO NPs against *S. aureus* and *E. coli* at 1000 μg mL^{-1} were 11mm and 8 mm respectively. Furthermore, alcoholic extracts of plants have been found to have more antibacterial properties than aqueous extracts [56]. In another research revealed that the ethanolic extract of *H. perforatum* exhibited a stronger antibacterial activity against *E. faecalis* and *s. aureus PTCC 1112* compared to certain Gram-negative bacteria [78]. Different potential antimicrobial mechanisms have been reported to demonstrate the inhibitory effects of ZnO NPs against tested bacteria. Some of the proposed mechanisms can be described as follows: (a) ZnO nanoparticles can be dissolved into the cell and then zinc ions can be released. At the cellular level, Zn ions may attach to the bacterial membrane and change its permeability, causing leakage of proteins and sugars and ultimately cell death. (b) Small particle size and ROS generation are important parameters affecting the antimicrobial activity of ZnO NPs. The production ROS damages the vital components which are necessary for sustaining the expected physiological functions of the bacteria, causes cell death [76]. To induce cell death, the ZnO nanomaterial should amassed and penetrate into the protoplasm of bacterial cell [79]. The mean size of the phyto-fabricated ZnO NPs is relatively 14 nm and also semi-spherical shaped, that revealed exceptional antibacterial activity.

3.6.2. MIC and MBC evaluation

The Minimum Inhibitory Concentration (MIC) values of bio-fabricated ZnO NPs and plant extract were obtained against different bacterial strains and the achieved outcomes are reported in Table 2. The MIC values of *H. perforatum*/ZnO NPs against *MRSA*, *B. subtilis* and *P. aeruginosa* were 156.2, 39.06 and 625 μg/mL orderiy. Also aqueous extract of *H. perforatum* exhibited inhibitory activity against *MRSA* and *B. subtilis* (MIC 2500 μg/mL). The obtained MIC values were in accord with the findings of Mahendra et al. [77] and Gilavand et al. [80] studies. These studies showed that the MIC values of phytosynthesized zinc oxide nanoparticles were obtained at lower concentrations compared to the plant extract, indicating their stronger antibacterial activity. The research also shows that organic solvents are more appropriate than water for the extraction of antibacterial compounds from plants [81]. Additionally, a great antimicrobial activity of methanol extracts of *H. Perforatum* against typical Gram-positive bacteria with MIC values of 50 μg mL^{-1} was reported by Conforti et al. [82]. These observations of treatment with *H. perforatum*/ZnO NPs can be due to numerous biological interactions. Furthermore, many ROS produced by the use of ZnO nanoparticles can cause membrane damage and cell death [83]. Minimum bactericidal concentration (MBC) complements the MIC value. According to Table 2, the MBC values of ZnO nanoparticles against *B. subtilis*, *MRSA* and *P. aeruginosa* were 78.12, 312.5 and 625 μg/mL, orderly. *H. perforatum*/ZnO NPs had adequate antibacterial activity against the Gram-positive strain. Our research indicates that phytosynthesized ZnO NPs can be applied as potential antimicrobial factor to treat difficulties induced by the studied bacteria.

4. Conclusion

It is widely known that the fabrication of Zinc oxid NPs mediated by plant extract is much more cost-effective and safer, that too according to green chemistry guidelines. Phytosynthesis of ZnO nanomaterials via aqueous extract of *H. perforatum* as capping and stabilizing agents was reported and structurally determined employing XRD, FT-IR, FESEM, TEM, EDS/Map, and UV-Vis DRS analyses. The fabricated ZnO NPs were semi-spherical shaped, monodisperse, with an average size of 14 nm, narrow size distribution, crystalline and pure phase, and also represented UV-Vis absorption at 365 nm. Furthuremore**,** the antibacterial activity of both the phytosynthesized ZnO NPs and the extract was investigated against *MRSA*, *P. aeruginosa* and *B. subtilis* using the agar disc diffusion method, MBC and Broth micro-dilution method to determine MIC. The results revealed that the antibacterial properties of *H. perforatum*/ZnO NPs and extract against Gram-positive bacteria are higher than against Gram-negative bacteria. The obtained findings in this research proposed that the phyto-fabricated ZnO NPs have suitable biological characteristic, including antimicrobial potential that can be applied in various medicinal and biological utilizations.

Acknowledgements

We express our heartfelt gratitude to the Department of Organic Chemistry, Faculty of Pharmaceutical Chemistry, Tehran Medical Sciences, Islamic Azad University, Tehran, Iran for their assistance in this research.

References

[1] K.V. Dhandapani, D. Anbumani, A.D. Gandhi, P. Annamalai, B.S. Muthuvenkatachalam, P. Kavitha and B. Ranganathan, Green route for the synthesis of zinc oxide nanoparticles from Melia azedarach leaf extract and evaluation of their antioxidant and antibacterial activities. *Biocatal. Agric. Biotechnol.*, 24 (2020) 101517.

[2] S. Ahmed, S. A. Chaudhry and S. Ikram, A review on biogenic synthesis of ZnO nanoparticles using plant extracts and microbes: a prospect towards green chemistry. *J. Photochem. Photobiol. B: Biol.*, 166 (2017) 272–284.

[3] K.E. Yunusov, A.A. Atakhanov, N.S. Ashurov, A.A. Sarymsakov and S.S. Rashidova, Physicochemical studies of cotton cellulose and its derivatives containing silver nanoparticles. *Chem. Nat. Compd.*, 47 (2011) 415-418.

[4] M.S. Chavali and M.P. Nikolova, Metal oxide nanoparticles and their applications in nanotechnology. *SN Appl. Sci.*, 1(2019) 607.

[5] A. Cartwright, K. Jackson, C. Morgan, A. Anderson and D.W. Britt, A review of metal and metal-oxide nanoparticle coating technologies to inhibit agglomeration and increase bioactivity for agricultural applications. *Agron.*, 10 (2020)1018.

[6] Ü. Özgür, Y.I. Alivov, C. Liu, A. Teke, M.A. Reshchikov, S. Doğan, V. Avrutin, S. J. Cho and Morkoç, A comprehensive review of ZnO materials and devices. *J. Appl. Phys.*, 98 (2005) 041301.

[7] M.A. Borysiewicz, ZnO as a functional material, a review. *Crystals.*, 9 (2019) 505.

[8] G. Lavanya, T. Suvarna and C. Vardhani, Structural and Optical Properties of (MgZnO/rGO) Nanocomposites. *J. Chem. Lett.*, 4 (2023) 136-147.

[9] M. Thirumavalavan, K. L. Huang and J.F. Lee, Preparation and morphology studies of nano zinc oxide obtained using native and modified chitosans. *Materials.*, 6 (2013) 4198-4212.

[10] H. Agarwal, S.V. Kumar and S. Rajeshkumar, A review on green synthesis of zinc oxide nanoparticles–An eco-friendly approach. *Resour -Effic Technol.*, 3 (2017) 406-413.

[11] A. Król, P. Pomastowski, K. Rafińska, V. Railean-Plugaru and B. Buszewski, Zinc oxide nanoparticles: Synthesis, antiseptic activity and toxicity mechanism. *Adv. Colloid. Interface Sci.*, 249 (2017) 37-52.

[12] K. Parveen, V. Banse and L. Ledwani, Green synthesis of nanoparticles: their advantages and disadvantages. In AIP conference proceedings. in: AIP conference proceedings, *AIP Publishing LLC.*, 1724 (2016) 020048.

[13] O.V. Kharissova, H.R. Dias, B.I. Kharisov, B.O. Pérez and V.M.J. Pérez, The greener synthesis of nanoparticles. *Trends Biotechnol.*, 31(2013) 240-248.

[14] I. Hussain, N.B. Singh, A. Singh, H. Singh and S.C. Singh, Green synthesis of nanoparticles and its potential application. *Biotechnol. Lett.*, 38 (2016) 545-60.

[15] A. Raja, S. Ashokkumar, R.P. Marthandam, J. Jayachandiran, C.P. Khatiwada, K. Kaviyarasu, R.G. Raman and M. Swaminathan, Eco-friendly preparation of zinc oxide nanoparticles using Tabernaemontana divaricata and its photocatalytic and antimicrobial activity. *J. Photochem. Photobiol. B: Biol.*, 181(2018)53-58.

[16] H. Mohd Yusof, R. Mohamad, U.H. Zaidan and A. Rahman, Microbial synthesis of zinc oxide nanoparticles and their potential application as an antimicrobial agent and a feed supplement in animal industry: a review. *J. Anim. Sci. Biotechnol.*, 10 (2019) 1-22.

[17] B. Sumanth, T.R. Lakshmeesha, M.A. Ansari, M.A. Alzohairy, A.C. Udayashankar, B. Shobha, S.R. Niranjana, C. Srinivas and A. Almatroudi, Mycogenic synthesis of extracellular zinc oxide nanoparticles from Xylaria acuta and its nanoantibiotic potential. *Int. J. Nanomedicine.*, 15 (2020) 8519.

[18] V. Kalpana and V. Devi Rajeswari, A review on green synthesis, biomedical applications, and toxicity studies of ZnO NPs. *Bioinorg.Chem. Appl.*, 2018 (2018).

[19] J. Osuntokun, D.C. Onwudiwe and E.E. Ebenso, Green synthesis of ZnO nanoparticles using aqueous Brassica oleracea L. var. italica and the photocatalytic activity. *Green Chem. Lett. Rev.*, 12 (2019) 444-457.

[20] A.K. Singh, P. Pal, V. Gupta, T.P. Yadav, V. Gupta and S.P. Singh, Green synthesis, characterization and antimicrobial activity of zinc oxide quantum dots using Eclipta alba. *Mater. Chem. Phys.*, 203 (2018) 40-48.

[21] P. Singh, Y.J. Kim, D. Zhang and D.C. Yang, Biological synthesis of nanoparticles from plants and microorganisms. *Trends Biotechnol.*, 34(2016) 588-599.

[22] C. Vidya, S. Hiremath, M.N. Chandraprabha, M.L. Antonyraj, I.V. Gopal, A. Jain and K. Bansal, Green synthesis of ZnO nanoparticles by Calotropis gigantea. *Int. J. Curr. Eng. Technol.*, 1(2013) 118-120.

[23] S. Waseem, T. Sittar, Z.N. Kayani, S. Gillani, M. Rafique, M.A. Nawaz, S.M. Shaheen and M.A. Assiri, Plant mediated green synthesis of zinc oxide nanoparticles using Citrus jambhiri lushi leaves extract for photodegradation of methylene blue dye. *Physica B Condens Matter.*, 663(2023) 415005.

[24] K. Dulta, G. Koşarsoy Ağçeli, P. Chauhan, R. Jasrotia and P. Chauhan, A novel approach of synthesis zinc oxide nanoparticles by Bergenia ciliata rhizome extract: antibacterial and anticancer potential. *J. Inorg. Organomet. Polym. Mater.* 31(2021) 180-190.

[25] S.N.A.M. Sukri, K. Shameli, M.M. Wong, S.Y. Teow, J. Chew and N.A. Ismail, Cytotoxicity and antibacterial activities of plant-mediated synthesized zinc oxide (ZnO) nanoparticles using Punica granatum (pomegranate) fruit peels extract. *J. Mol. Struct.*, 1189 (2019) 57-65.

[26] K. Velsankar, S. Sudhahar, G. Parvathy and R. Kaliammal, Effect of cytotoxicity and antibacterial activity of biosynthesis of ZnO hexagonal shaped nanoparticles by Echinochloa frumentacea grains extract as a reducing agent. *Mater. Chem. Phys.*, 239 (2020) 121976.

[27] M. Bandeira, A.L. Possan, S.S. Pavin, C.S. Raota, M.C. Vebber, M. Giovanela, M. Roesch-Ely, D.M. Devine and J.S. Crespo, Mechanism of formation, characterization and cytotoxicity of green synthesized zinc oxide nanoparticles obtained from Ilex paraguariensis leaves extract. *Nano-Struct. Nano-Objects.*, 24 (2020) 100532.

[28] S. Dawar, D. Mehta and B.K. Mehta, Phyto assisted Synthesis and Comparative Studies of Zinc Oxide Nanoparticles with Ficus benghalensis from Conventional Heating and Microwave Heating Method. *J. Chem. Lett,* (2023) , in press.

[29] H. Sadiq, F. Sher, S. Sehar, E.C. Lima, S. Zhang, H.M. Iqbal, F. Zafar and M. Nuhanović, Green synthesis of ZnO nanoparticles from Syzygium Cumini leaves extract with robust photocatalysis applications. *J. Mol. Liq.*, 335 (2021) 116567.

[30] M. Anbuvannan, M. Ramesh, G. Viruthagiri, N. Shanmugam and N. Kannadasan, Synthesis, characterization and photocatalytic activity of ZnO nanoparticles prepared by biological method. *Spectrochim. Acta A Mol Biomol. Spectrosc.*, 143 (2015) 304-308.

[31] S. Ahmed, SA. Chaudhry and S. Ikram, A review on biogenic synthesis of ZnO nanoparticles using plant extracts and microbes: a prospect towards green chemistry. *J. Photochem. Photobiol. B.*,166 (2017) 272-284.

[32] A. Singh, NÁ. Singh, S. Afzal, T. Singh and I. Hussain, Zinc oxide nanoparticles: a review of their biological synthesis, antimicrobial activity, uptake, translocation and biotransformation in plants. *J. Mater. Sci.*, 53 (2018) 185-201.

[33] S. Chaudhary, A. Umar, K.K. Bhasin and S. Baskoutas, Chemical sensing applications of ZnO nanomaterials. *Materials*, 11(2):287. Materials. 11(2018) 287.

[34] S.E. Cross, B. Innes, M.S. Roberts, T. Tsuzuki, T.A. Robertson and P. McCormick, Human skin penetration of sunscreen nanoparticles: in vitro assessment of a novel micronised zinc oxide formulation. *Skin Pharmacol. Physiol.*, 20(2007), 148-154.

[35] T. Mishchenko, E. Mitroshina, I. Balalaeva, O. Krysko, M. Vedunova and D. Krysko, An emerging role for nanomaterials in increasing immunogenicity of cancer cell death.Biochim. Biophys. *Acta Rev. Canc.*, 1871(2019) 99-108.

[36] V. Houskova, V. Stengl, S. Bakardjieva, N. Murafa and A. Kalendova, Oplustil F Zinc oxide prepared by homogeneous hydrolysis with thioacetamide, its destruction of warfare agents, and photocatalytic activity. *J. Phys. Chem. A*, 111(2007) 4215-21.

[37] R. Dadi, R. Azouani, M. Traore, C. Mielcarek and A. Kanaev, Antibacterial activity of ZnO and CuO nanoparticles against gram positive and gram negative strains. *Mater. Sci. Eng. C Mater. Biol. Appl.*, 104 (2019) 109968.

[38] V.D. Rosenthal, S. Guzman and P.W. Orellano, Nosocomial infections in medical-surgical intensive care units in Argentina: Attributable mortality and length of stay. *Am. J. Infect. Control.*, 31(2003) 291-295.

[39] P. Kumar, P. Huo, R. Zhang and B. Liu, Antibacterial properties of graphene-based nanomaterials. *Nanomaterials*, 9 (2019) 737.

[40] M. Sheydaei, S. Shahbazi-Ganjgah, E. Alinia-Ahandani, M. Sheidaie and M. Edraki, An overview of the use of plants, polymers and nanoparticles as antibacterial materials. *Chem. Rev. Lett.*, 5 (2022) 207-216.

[41] S. Sherzad Othman and M. Noori Abdollah, Synthesis of Novel Michael Adducts and Study of their Antioxidant and Antimicrobial Activities. *Chem. Rev. Lett.*, 5 (2022) 226-233.

[42] A.K.O. Aldulaimi, A.H. Idan, A.A. Majhool, M.J. Jawad, Z.H. Khudhair, S.M. Hassan and S.S.S.A. Azziz, Synthesis of new antibiotic agent based on mannich reaction. *Int. J. Drug Deliv. Tec.*, 12 (2022) 1428-1432.

[43] A.K.O. Aldulaimi, M.J. Jawad, S.M. Hassan, T.S. Alwan, S.S.S.A. Azziz and Y.M. Bakri, The potential antibacterial activity of a novel amide derivative against gram-positive and gram-negative bacteria. *Int. J. Drug Deliv. Tec.*, 12 (2022) 510-515.

[44] A.K.O. Aldulaim, N.M. Hameed, T.A. Hamza and A.S. Abed, The antibacterial characteristics of fluorescent carbon nanoparticles modified silicone denture soft liner. *J. Nanostruct.*, 12 (2022) 774-781.

[45] S.A. Siadati, M. Afzali and M. Sayyadi, Could silver nano-particles control the 2019-nCoV virus?; An urgent glance to the past. *Chem. Rev. Lett.*, 3 (2020) 9-11.

[46] K.E. Yunusov, A.A. Sarymsakov, S.V. Mullajonova, F.M. Turakulov and S.S. Rashidova, Bactericidal effect of cotton fabric treated with polymer solution containing silver nanoparticles of different sizes and shapes. *Asian J. Chem.*, 32 (2020) 1335-1342.

[47] K.E. Yunusov, A.A. Sarymsakov and S.S. Rashidova, Structure and properties of biodegradable carboxymethyl cellulose films containing silver nanoparticles. *Polym. Sci., Ser. A*, 56 (2014) 283-288.

[48] K.E. Yunusov, A.A. Sarymsakov, J.Z.O. Jalilov and A.A.o. Atakhanov, Physicochemical properties and antimicrobial activity of nanocomposite films based on carboxymethylcellulose and silver nanoparticles. *Polym. Adv. Technol.*, 32 (2021) 1822-1830.

[49] S.V. Gudkov, D.E. Burmistrov, D.A. Serov, M.B. Rebezov, A.A. Semenova and A.B. Lisitsyn, A mini review of antibacterial properties of ZnO nanoparticles. *Front. Phys.*,9 (2021) 641481.

[50] A.M. Pillai, V.S. Sivasankarapillai, A. Rahdar, J. Joseph, F. Sadeghfar, K. Rajesh and G.Z. Kyzas, Green synthesis and characterization of zinc oxide nanoparticles with antibacterial and antifungal activity. *J. Mol. Struct.*, 1211 (2020) 128107.

[51] M. Edraki, I. Mousazadeh Moghaddampour, M. Banimahd Keivani and M. Sheydaei, Characterization and

antimicrobial properties of Matcha green tea. *Chem. Rev. Lett.*, 5 (2022) 76-82.

[52] S.S.S.A. Azziz, A.K.O. Aldulaimi, S.A. Aowda, Y.M. Bakri, A.A. Majhool, R.M. Ibraheem and F. Abdullah, Secondary metabolites from leaves of polyalthia lateriflora and their antimicrobial activity. *Int. J.Res. Pharm. Sci.* 11 (2020) 4353-4358.

[53] E.C. Emenike and C. Onyema, Phytochemical, Heavy Metals and Antimicrobial Study of the Leaves of Calopogonium mucunoides, *J. Chem. Lett.*, 3 (2022) 30-37.

[54] A.K.O. Aldulaimi, A.H. Idan, A.H. Radhi, S.A. Aowda, S.S.S.A. Azziz, W.M.N.H. W. Salleh, T.K.O. Aldulaimi and N.A.M. Ali, Gcms analysis and biological activities of iraq zahdi date palm phoenix dactylifera L volatile compositions. *Res. J. Pharm. Tec.*, 13 (2020) 5207-5209.

[55] E. Sharafi, S.M. Khayam Nekoei, M.H. Fotokian, D. Davoodi and H. Loo, Improvement of hypericin and hyperforin production using zinc and iron nano-oxides as elicitors in cell suspension culture of St John's wort (Hypericum perforatum L.). *J. medicinal plants by-products.*, 2 (2013) 177-184.

[56] Z. Saddiqe, I. Naeem and A. Maimoona, A review of the antibacterial activity of Hypericum perforatum L. *J. Ethnopharmacol.*, 131(2010) 511-21.

[57] J. Asgarpanah, Phytochemistry, pharmacology and medicinal properties of Hypericum perforatum L. *Afr. J. Pharmacy Pharmacol.*, 6 (2012) 1387-1394.

[58] A. Alahmad, A. Feldhoff, N.C. Bigall, P. Rusch, T. Scheper and J.G. Walter, Hypericum perforatum L. mediated green synthesis of silver nanoparticles exhibiting antioxidant and anticancer activities. *Nanomater.*, 11(2021) 487.

[59] B.A. Silva, F. Ferreres, J.O. Malva and A.C. Dias, Phytochemical and antioxidant characterization of Hypericum perforatum alcoholic extracts. *Food Chem.*, 90 (2005) 157-167.

[60] M. Bandeira, M. Giovanela, M. Roesch-Ely, D.M. Devine and J.S. Crespo, Green synthesis of zinc oxide nanoparticles: A review of the synthesis methodology and mechanism of formation. *Sustain Chem. Pharm.*, 15 (2020) 100223.

[61] G. K. Weldegebrieal, Synthesis method, antibacterial and photocatalytic activity of ZnO nanoparticles for azo dyes in wastewater treatment: A review, *Inorg. Chem. Commun.*, 120 (2020) 108140.

[62] C.A. Soto-Robles, P.A. Luque, C.M. Gómez-Gutiérrez, O. Nava, A.R. Vilchis-Nestor, E. Lugo-Medina, R. Ranjithkumar and A. Castro-Beltrán, Study on the effect of the concentration of Hibiscus sabdariffa extract on the green synthesis of ZnO nanoparticles, *Results Phys.* 15 (2019) 102807.

[63] F.M. Mohammadi and N. Ghasemi, Influence of temperature and concentration on biosynthesis and characterization of zinc oxide nanoparticles using cherry extract, *J. Nanostruct. Chem.* 8 (2018) 93–102.

[64] S. Nagarajan and K.A. Kuppusamy, Extracellular synthesis of zinc oxide nanoparticle using seaweeds o f gulf of Mannar , India, *J. Nanobiotechnology* 11 (2013) 1–11.

[65] S. Azizi, R. Mohamad, A. Bahadoran, S. Bayat, R.A. Rahim, A. Ariff and W.Z. Saad, Effect of annealing temperature on antimicrobial and structural properties of biosynthesized zinc oxide nanoparticles using flower extract of Anchusa italica, *J.Photochem. Photobiol. B: Biol.* 161 (2016) 441–449.

[66] S. Jafarirad, M. Mehrabi, B. Divband and M. Kosari-Nasab, Biofabrication of zinc oxide nanoparticles using fruit extract of Rosa canina and their toxic potential against bacteria: A mechanistic approach. Mater. Sci. Eng. C., 59 (2016) 296–302.

[67] S.J. Flora, Structural, chemical and biological aspects of antioxidants for strategies against metal and metalloid exposure. Oxid. Med. Cell Longev., 2 (2009) 191-206.

[68] B.Y. Ting, N.K. Fuloria, V. Subrimanyan, S. Bajaj, S.V. Chinni, L.V. Reddy, K.V. Sathasivam, S. Karupiah, R. Malviya, D.U. Meenakshi and N. Paliwal, Biosynthesis and Response of Zinc Oxide Nanoparticles against Periimplantitis Triggering Pathogens. *Materials*, 15 (2022) 3170.

[69] E.G. Goh, X. Xu and P.G. McCormick, Effect of particle size on the UV absorbance of zinc oxide Nanoparticles. *Scr. Mater.*, 78 (2014) 49-52.

[70] G. Sharmila, M. Thirumarimurugan and C. Muthukumaran, Green synthesis of ZnO nanoparticles using Tecoma castanifolia leaf extract: characterization and evaluation of its antioxidant, bactericidal and anticancer activities. *Microchem. J.*, 145 (2019) 578-587.

[71] M.J. Akhtar, M. Ahamed, S. Kumar, M.M. Khan, J. Ahmad and S.A. Alrokayan, Zinc oxide nanoparticles selectively induce apoptosis in human cancer cells through reactive oxygen species. *Int. J. Nanomedicine.*, 7 (2012) 845-857.

[72] L.P. Etcheverry, W.H. Flores, D.L. Silva and E.C. Moreira, Annealing effects on the structural and optical properties of ZnO nanostructures. *Mat. Res.*, 21(2018) e20170936.

[73] D. Church, S. Elsayed, O. Reid, B. Winston and R. Lindsay, Burn wound infections. *Clin. Microbiol. Rev.*, 19(2006) 403-434.

[74] A. Sirelkhatim, S. Mahmud, A. Seeni, N. H. M. Kaus, L. C. Ann, S. K. M. Bakhori and D. Mohamad, Review on zinc oxide nanoparticles: antibacterial activity and toxicity mechanism, *Nanomicro Lett.*, 7 (2015) 219-242.

[75] K. M. Reddy, K. Feris, J. Bell, D. G. Wingett, C. Hanley and A. Punnoose, Selective toxicity of zinc oxide nanoparticles to prokaryotic and eukaryotic systems, *Appl. Phys. Lett.*, 90 (2007) 1–8.

[76] A. Ahmadi Shadmehri and F. Namvar, A review on green synthesis, cytotoxicity mechanism and antibacterial activity of Zno NPs. *J. Basic Res. Med. Sci.*, 1(2020) 23-31.

[77] C. Mahendra, M.N. Chandra, M. Murali, M.R. Abhilash, S.B. Singh, S. Satish and M.S. Sudarshana, Phyto-fabricated ZnO nanoparticles from Canthium dicoccum

(L.) for antimicrobial, anti-tuberculosis and antioxidant activity. *Process. Biochem.*, 89 (2020) 220-226.
[78] M. Mazandarani, S. Yassaghi, M.B. Rezaei, A.R. Mansourian and E.O. Ghaemi, Ethnobotany and antibacterial activities of two endemic species of Hypericum in North-East of Iran. *Asian J. Plant Sci.*, (2007).
[79] L. Wang, C. Hu and L. Shao, The antimicrobial activity of nanoparticles: present situation and prospects for the future. *Int. J. Nanomedicine.*, 12 (2017)1227.
[80] F. Gilavand, R. Saki, S.Z. Mirzaei, H. Esmaeil Lashgarian, M. Karkhane and A. Marzban, Green synthesis of zinc nanoparticles using aqueous extract of Magnoliae officinalis and assessment of its bioactivity potentials. *Biointerface. Res. Appl. Chem.*, (2020).
[81] C. Barbagallo and G. Chisari, Antimicrobial activity of three Hypericum species. *Fitoterapia*, 58 (1987) 175-177.
[82] F. Conforti, G.A. Statti, R. Tundis, A. Bianchi, C. Agrimonti, G. Sacchetti, E. Andreotti, F. Menichini and F. Poli, Comparative chemical composition and variability of biological activity of methanolic extracts from Hypericum perforatum L. *Nat. Prod. Res.*, 19 (2005) 295-303.
[83] K. Gold, B. Slay, M. Knackstedt and A.K. Gaharwar, Antimicrobial activity of metal and metal-oxide based nanoparticles. *Adv. Ther.*, 1 (2018) 1700033.